Solid State Nuclear Magnetic Resonance 45–46 (2012) 51–58

Contents lists available at SciVerse ScienceDirect

Solid State Nuclear Magnetic Resonance

journal homepage: www.elsevier.com/locate/ssnmr

Intramolecular ^{1}H–^{13}C distance measurement in uniformly ^{13}C, ^{15}N labeled peptides by solid-state NMR

Shenhui Li [a,b,*], Yongchao Su [b,**], Mei Hong [b]

[a] Wuhan Institute of Physics and Mathematics, the Chinese Academy of Sciences, Wuhan 430071, China
[b] Department of Chemistry, Iowa State University, Ames, IA 50011, United States

ARTICLE INFO

Article history:
Received 9 January 2012
Received in revised form
29 April 2012
Accepted 5 June 2012
Available online 15 June 2012

Keywords:
REDOR
Distance measurement
Simulation
Dihedral angles

ABSTRACT

A ^{1}H–^{13}C frequency-selective REDOR (FS-REDOR) experiment is developed for measuring intramolecular ^{1}H–^{13}C distances in uniformly ^{13}C, ^{15}N-labeled molecules. Theory and simulations show that the experiment removes the interfering homonuclear ^{1}H–^{1}H, ^{13}C–^{13}C and heteronuclear ^{1}H–^{15}N, ^{13}C–^{15}N dipolar interactions while retaining the desired heteronuclear ^{1}H–^{13}C dipolar interaction. Our results indicate that this technique, combined with the numerical fitting, can be used to measure a ^{1}H–^{13}C distance up to 5 Å. We also demonstrate that the measured intramolecular ^{1}H–^{13}C distances are useful to determine dihedral angles in proteins.

1. Introduction

High-resolution magic-angle-spinning solid-state NMR (SSNMR) spectroscopy has become a complementary method to X-ray crystallography and solution NMR for determining three-dimensional structures of proteins. This structure determination relies on the measurement of torsion angles and distances[1] and orientational constraints using aligned samples[2,3]. Backbone ^{13}C and ^{15}N chemical shifts are well known to be sensitive to protein (ϕ, ψ) torsion angles, and can be measured straightforwardly to constrain the protein secondary structure [4–6]. In addition to chemical shifts, a number of heteronuclear dipolar-correlation techniques such as HNCH [7], NCCN [8] and HCCH [9,10] have been developed to quantitatively measure the backbone and sidechain dihedral angles.

Solid state NMR has been proven to be a reliable technique to obtain the quantitative distance information in various systems [11–25]. Distances between non-proton atoms in proteins can be measured using 2D and 3D correlation experiments such as DARR [26], RFDR [20], CHHC [27], PAR [28], R^2W [29], FS-REDOR [30] and ZF-TEDOR [31]. Homonuclear correlation experiments such as DARR and CHHC yield qualitative ^{13}C–^{13}C or ^{15}N–^{15}N distance constraints based on the growth of cross peak intensities as a function of mixing time: short distances manifest as fast build-up curves whereas long-range distances exhibit slow build-up curves. Alternatively, the rotational resonance width (R^2W) experiment [29,32,33] yields more quantitative ^{13}C–^{13}C distance constraints by monitoring cross peak intensities as a function of MAS frequency while the spin diffusion mixing time is held constant. To determine heteronuclear distances, one can use the frequency-selective (FS) REDOR experiment [30] or the 3D ZF (zero-filter) TEDOR experiment [31]. These methods have so far been applied mostly to ^{13}C–^{15}N distance determination in proteins [34,35].

While heavy-atom ^{13}C–^{13}C, ^{13}C–^{15}N and ^{15}N–^{15}N distances are important for protein structure determination, distances involving protons, such as ^{1}H–^{13}C and ^{1}H–^{15}N distances, also provide valuable constraints to the backbone and sidechain conformation of proteins. The difficulty presented by the dense multi-spin network of protons in proteins was recently shown to be possibly overcome using a Y-nucleus detected ^{1}H-X REDOR [11] technique [36,37,38], where X and Y represent two different types of nuclei. For example, a ^{15}N-detected ^{1}H–^{13}C REDOR experiment allows the measurement of the distance of a carbonyl carbon to an amide proton involved in N–H…O=C hydrogen bond. However, the Y-detected ^{1}H-X REDOR experiment has the limitation that it requires the samples to be site-specifically labeled in the X nucleus in order to avoid the complication of multiple X nuclei simultaneously coupled to each ^{1}H spin. It is thus desirable to extend the technique to uniformly ^{13}C, ^{15}N labeled proteins to measure multiple ^{1}H–^{13}C distances.

* Corresponding author at: Wuhan Institute of Physics and Mathematics, the Chinese Academy of Sciences, Wuhan 430071, China.
** Corresponding author. Present address: Francis Bitter Magnet Laboratory, Department of Chemistry, Massachusetts Institute of Technology, Cambridge, MA 02139, United States.
E-mail addresses: lishenhui@wipm.ac.cn (S. Li), ycsu@mit.edu (Y. Su).

0926-2040/$ - see front matter © 2012 Elsevier Inc. All rights reserved.
http://dx.doi.org/10.1016/j.ssnmr.2012.06.001

In this work, we describe the theory, simulation and application of a ^{13}C-detected FS-REDOR experiment to extract ^{1}H–^{13}C distances. By using frequency-selective REDOR, we not only extend the ^{1}H-X REDOR principle to uniformly ^{13}C, ^{15}N-labeled samples but also show that the allowance of ^{13}C detection rather than ^{15}N detection in the previous study[36–38] significantly increases the sensitivity of this approach. The feasibility of our ^{1}H–^{13}C FS-REDOR experiment has been evaluated on two ^{13}C, ^{15}N-labeled model compounds, formyl-Met-Leu-Phe-OH (f-MLF) and histidine.

2. Experimental

2.1. Materials

Uniformly ^{13}C, ^{15}N-labeled f-MLF was purchased from Cambridge Isotope Laboratories and used without further purification. 98% ^{13}C, ^{15}N-labeled Histidine·HCl·H_2O was purchased from Sigma-Aldrich and was diluted to 20% by codissolving with 80% unlabeled histidine to remove the interfering intermolecular dipolar couplings. The mixture was recrystallized at pH 8.0 as described before.[39] The solid-state NMR structure of f-MLF (PDB code: 1Q7O) [40] was referenced to compare with the measured distances. For histidine, the measured intramolecular ^{1}H–^{13}C distances and deduced sidechain dihedral angles were compared with the values in the crystal structure of L-histidine (CSD code: LHISTD02).

2.2. Instrumentation

Solid-state NMR experiments were carried out on a wide-bore Bruker AVANCE-600 spectrometer using a double-resonance 4-mm MAS probe. Samples were spun at 5.0 kHz at room temperature for all experiments. Typical radiofrequency field strengths were 50–63 kHz for ^{13}C and 62 − 83 kHz for ^{1}H. ^{13}C chemical shifts was referenced to the α-Gly C' signal at 176.49 ppm on the TMS scale.

3. Results and discussion

3.1. ^{1}H–^{13}C FS-REDOR experiment

Fig. 1 illustrates the pulse sequence for the ^{1}H–^{13}C FS-REDOR experiment. After an initial 90° pulse and a magic-angle pulse of 54.7° (θ_m), the ^{1}H magnetization is tilted to the $-x$ direction, perpendicular to the effective field direction of the subsequent Frequency Switched Lee-Goldburg (FSLG) [41,42] pulses, which remove the ^{1}H–^{1}H homonuclear coupling [43–45]. ^{1}H magnetization evolves under the interactions of the ^{1}H chemical shift and ^{1}H–^{13}C dipolar coupling for 2N rotor periods with a total duration of τ_m. The ^{1}H–^{13}C dipolar interaction is recoupled under MAS by two symmetric π-pulse trains, which contain two ^{13}C pulses per rotor period. A rectangular selective ^{13}C π pulse is applied in the middle of ^{1}H–^{13}C dipolar recoupling to selectively refocus the ^{13}C spins of interest. Synchronously on ^{1}H channel, a WIM-24 pulse train [46] is applied to remove the residual homonuclear ^{1}H–^{1}H and heteronuclear ^{1}H–^{13}C dipolar couplings under MAS. In the middle of WIM-24 decoupling, a π pulse of 6.1 μs was applied to recouple the ^{1}H–^{13}C dipolar interaction. The rest ^{1}H–^{1}H decoupling during the middle two rotor periods is achieved by using FSLG pulses. We used a ^{13}C selective π pulse of 320 μs, which is supposed to selectively invert a ^{13}C frequency range of around 6 ppm, considering the ^{13}C Larmor frequency of 150 MHz in our study.

In order to detect the dipolar modulation of the ^{1}H spins by observing the resolved ^{13}C intensity, the ^{1}H magnetization is transferred to the coupled ^{13}C spin through a short, 40 μs, Lee-Goldberg cross-polarization (LG-CP) period, which eliminates the possible ^{1}H spin diffusion. The effective spin-lock field strength of LG-CP is 62.5 kHz. In the REDOR mixing period, the effective field strength of the FSLG decoupling and the transverse field of the WIM-24 sequence is set to be 102.1 kHz and 81.7 kHz, respectively.

3.2. Theoretical background

We consider a multi-spin system consisting of m ^{13}C spins and n protons. In the ^{1}H–^{13}C FS-REDOR experiment, ^{13}C–^{13}C, ^{1}H–^{15}N and ^{13}C–^{15}N dipolar interactions commute with the ^{1}H chemical shift interaction and ^{1}H–^{13}C dipolar coupling, thus do not interfere the measurement of ^{1}H–^{13}C dipolar couplings. For directly bonded ^{1}H–^{13}C spin pairs, the ^{1}H–^{13}C J coupling is present, while the multi-bond ^{1}H–^{13}C J coupling is neglectable. Therefore, we only consider ^{1}H–^{13}C dipolar coupling and ^{13}C–^{13}C J coupling as the effective Hamiltonian in our FS-REDOR experiment:

$$H = \sum_{i=1}^{n}\sum_{j=1}^{m} \kappa\, \omega_{ij} 2I_{iz}S_{jz} + \sum_{k\neq j} \pi J_{jk} 2S_{jz}S_{kz} \tag{1}$$

Here J_{jk} is the ^{13}C–^{13}C scalar coupling between directly bonded j and k spins, and κ is the FSLG scaling factor for the ^{1}H–^{13}C dipolar coupling. ω_{ij} represents the ^{1}H–^{13}C dipolar coupling between the ^{1}H spin i and the ^{13}C spin j, and its value depends on the internuclear distance r_{ij} and orientation angles (θ, ϕ) of the dipolar vector relative to the magnetic field according to the following equation:

$$\omega_{ij} = \frac{\sqrt{2}}{\pi}\frac{\mu_0}{4\pi}\frac{\gamma_i\gamma_j}{r_{ij}^3}\sin 2\theta \sin\phi, \tag{2}$$

In the tilted frame of the FSLG sequence, the initial ^{1}H magnetization after the excitation pulses is $\rho(0)$:

$$\rho(0) = \sum_i p_i I_{ix}, \tag{3}$$

where p_i represents the initial polarization of the ith ^{1}H spin. The evolution of the ^{1}H magnetization under the effective

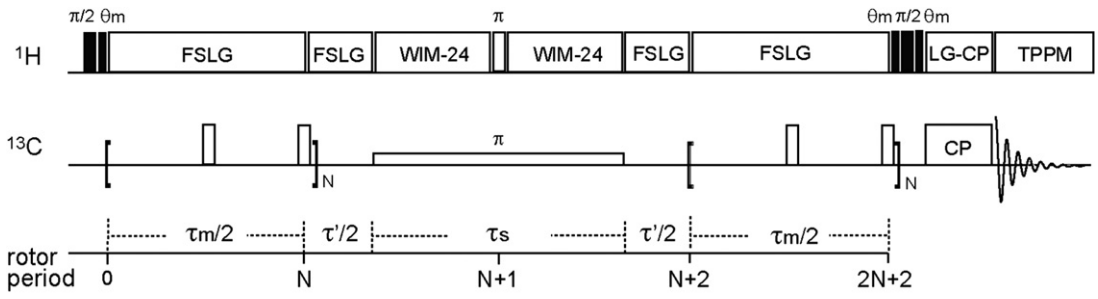

Fig. 1. Pulse sequence for ^{1}H–^{13}C frequency selective (FS) REDOR experiment.

Hamiltonian of Eq. (1) can be written as

$$\rho(\tau) = U(\tau)\rho(0)U(\tau)^{-1}, \tag{4}$$

where the propagator $U(\tau)$ is

$$\begin{aligned} U(\tau) = &\prod_{i,j}\exp -i\kappa\omega_{ij}(\tau_m/2)2I_{iz}S_{jz} \times \prod_{k\neq j}\exp -i\pi J_{jk}(\tau_m/2)2S_{jz}S_{kz} \\ &\times\prod_{i,j}\exp -i\kappa\omega_{ij}\tau_s 2I_{iz}S_{jz} \times \prod_{k\neq j}\exp -i\pi J_{jk}\tau_s 2S_{jz}S_{kz} \\ &\times\prod_{i,j}\exp -i\kappa\omega_{ij}(\tau_m/2)2I_{iz}S_{jz} \times \prod_{k\neq j}\exp -i\pi J_{jk}(\tau_m/2)2S_{jz}S_{kz}. \end{aligned} \tag{5}$$

In the above equation τ_m and τ_s represent the REDOR recoupling period and the ^{13}C selective-pulse period, respectively. Due to the WIM-24 decoupling, the scaling factor κ' and the effective coupling ω' during the ^{13}C selective-pulse period may be different from those of the rest of the REDOR mixing time. The ^{1}H density operator at the end of the whole recoupling period is

$$\begin{aligned} \rho(\tau_m) = \sum_i \Bigg\{ & p_i I_{ix} \prod_j \cos(\kappa\omega_{ij}\tau_m) \prod_{k\neq j}\cos(\pi J_{jk}\tau_m) \\ &\times \prod_j \cos\left(\kappa'\omega'_{ij}\tau_s\right) \prod_{k\neq j}\cos(\pi J_{jk}\tau_s) \Bigg\}. \end{aligned} \tag{6}$$

The first term represents the distance-dependent ^{1}H–^{13}C dipolar interaction. The second term represents ^{13}C–^{13}C J coupling which cannot be removed by hard π-pulses during the REDOR recoupling [30,47,48].Take ^{1}Hβ–^{13}Cα distance measurement for example, the one-bond $^{1}J_{CC}$ coupling of 55 Hz for ^{13}C′–^{13}Cα and 35 Hz for ^{13}Cα-^{13}Cβ [30,49] should be taken into account. The third term represents the selected ^{1}H–^{13}C dipolar interaction that is recoupled by the π-pulse trains. WIM-24 removes the ^{1}H–^{13}C dipolar interaction during the selective-pulse period, and the soft ^{13}C π pulse removes the J coupling between the ^{13}C spin of interest and its directly bonded ^{13}C, so the last two term can be ignored [50]. Therefore, the evolution of the ^{1}H density operator under the ^{1}H–^{13}C FS-REDOR pulse sequence can be simplified as

$$I_{ix} \xrightarrow{\kappa\omega_{ij}2I_{iz}S_{jz}} I_{ix}\cos(\kappa\omega_{ij}\tau_m) \xrightarrow{\pi J_{jk}2S_{jz}S_{kz}} I_{ix}\cos(\kappa\omega_{I_iS_j}\tau_m)\prod_{k\neq j}\cos(\pi J_{jk}\tau_m). \tag{7}$$

3.3. Numerical simulations of ^{1}H–^{13}C FS-REDOR dephasing

Numerical simulations were carried out to provide semi-quantitative analysis of the effects of various spin interactions on the ^{1}H–^{13}C REDOR dephasing in the ^{1}H–^{13}C FS-REDOR experiment. The REDOR curves were simulated using the SIMPSON software [51]. We first simulated the universal ^{1}H–^{13}C REDOR dephasing curves for several isolated ^{1}H–^{13}C spin pairs with distances of 1.1 Å, 2.1 Å and 4.0 Å, which correspond to the one-bond C–H distance, the two-bond C–H distance in a CH_2–CH_2 group, and a C–H spin pair separated by more than two bonds, respectively. The effective dipolar couplings for these distances are 13.22 kHz, 1.90 kHz, and 275 Hz, respectively, after taking into account the FSLG scaling factor. We then incorporated effects of FSLG homonuclear decoupling into the simulation, by using a spin system containing $^{1}H_2$–^{13}C with a ^{1}H–^{1}H homonuclear coupling of 22.6 kHz (1.75 Å) and a ^{1}H–^{13}C heteronuclear coupling of 3293 Hz (2.1 Å) and 477 Hz (4.0 Å). This three-spin system reasonably represents the ^{13}C$^{1}H_2$–^{13}C system. In the simulations, the ^{1}H 180° pulse in the middle of the C–H REDOR period was fixed to 10 μs, and the FSLG decoupling field was set to 100%, 90% and 80% of the intended field strength, allowing us to assess the effect of miscalibration of the ^{1}H FSLG pulse length during REDOR dephasing. Different experimental conditions were investigated separately to compare with the corresponding ^{1}H–^{13}C universal REDOR dephasing curves.

During the ^{13}C spin selection period, a soft ^{13}C π pulse with a pulse length equal to two rotor periods (400 μs) was applied on the ^{13}C channel in the middle of the REDOR period. This ^{13}C pulse was applied with or without ^{1}H WIM-24 decoupling. In addition, to simulate the real experimental condition, we also used a ^{13}C π pulse and a WIM-24 decoupling period of 320 μs and the rest part of two rotor periods was filled with FSLG. The REDOR dephasing curves for ^{1}H–^{13}C distances of 1.1 Å and 2.1 Å were simulated under these conditions and compared with the ideal REDOR dephasing curves, to exploit the effects of additional heteronuclear ^{1}H–^{13}C dipolar decoupling on the FS-REDOR experiment.

To examine the effect of one bond ^{13}C–^{13}C J coupling on the ^{1}H–^{13}C FS-REDOR dephasing curves, four spin systems containing $^{1}H_1$, $^{13}C_2$, $^{13}C_3$ and $^{13}C_4$ with J_{C2-C3} of 55 Hz (e.g. $^{13}C'$–$^{13}C_\alpha$) and J_{C2-C4} of 35 Hz (e.g. $^{13}C_\alpha$–$^{13}C_\beta$) [49] were inputted in the simulation program. Three different situations were considered in the ^{1}H–^{13}C FS-REDOR experiment: an ideal situation that both ^{13}C hard and soft π pulse can select $^{13}C_2$ out of $^{13}C_3$ and $^{13}C_4$; an actual situation that only ^{13}C soft π pulse can select $^{13}C_2$ out of $^{13}C_3$ and $^{13}C_4$; the third scenario with neither ^{13}C hard nor soft π pulse can select $^{13}C_2$ out of $^{13}C_3$ and $^{13}C_4$.

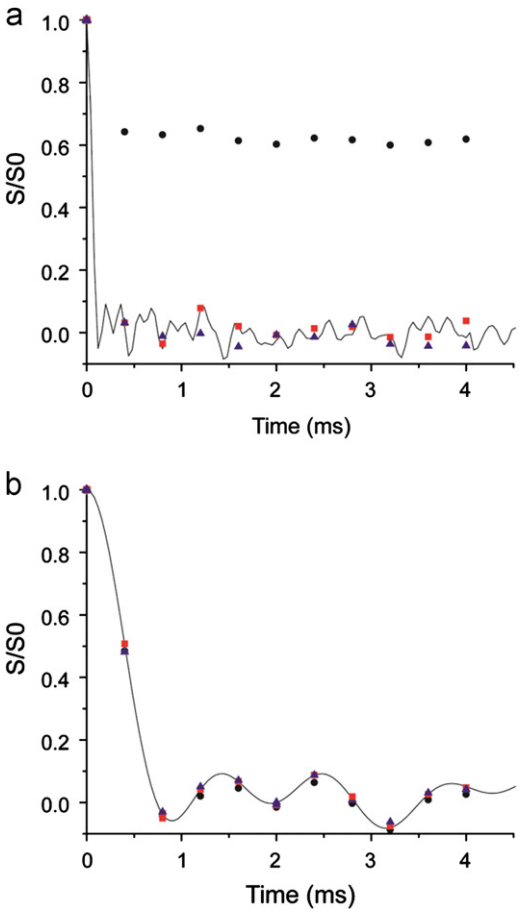

Fig. 2. REDOR simulations on ^{1}H–^{13}C heteronuclear decoupling in ^{1}H–^{13}C FS-REDOR experiment. In the simulation programs, two-spin systems containing $^{1}H_1$, $^{13}C_2$ with ^{1}H–^{13}C distances of 1.1 Å (a) and 2.1 Å (b) were selected. The control universal REDOR dephasing curves were depicted in black line. The dotted dephasing points in black (circle) represent ^{1}H–^{13}C REDOR condition without ^{1}H–^{13}C WIM-24 heteronuclear decoupling. The dotted dephasing points in red (square) and blue (triangle) represent ^{1}H–^{13}C REDOR condition with 400 and 320 μs ^{1}H–^{13}C WIM-24 heteronuclear decoupling. (For interpretation of the references to color in this figure legend, the reader is referred to the web version of this article.)

To fit the measured REDOR dephasing of f-MLF and histidine, we inputted heteronuclear ^{1}H–^{13}C dipolar coupling and one-bond ^{13}C–^{13}C J couplings of 55 Hz for $^{13}C'$–$^{13}C_{\alpha}$ and 35 Hz for $^{13}C_{\alpha}$–$^{13}C_{\beta}$.

3.4. Considerations of hetero- and homo-nuclear decoupling and scalar coupling during ^{1}H–^{13}C dipolar recoupling period

3.4.1. Effect of ^{1}H–^{13}C WIM heteronuclear decoupling

Fig. 2 shows ^{1}H–^{13}C REDOR dephasing with and without WIM-24 decoupling of the ^{1}H–^{13}C dipolar interaction during the selective ^{13}C pulse period. For the directly bonded ^{1}H–^{13}C spin pair, the universal ^{1}H–^{13}C REDOR curve decays to 0 by ~0.2 ms, as expected for the strong one-bond coupling. Afterwards, the S/S_0 value oscillates rapidly at around 0. When WIM-24 decoupling is turned off, the equilibrium dephasing value increases to about 0.60, largely differs from the ideal value of 0. While in the ^{1}H–^{13}C two-bond distances simulation, the simulated dephasing points were slightly deviated from the corresponding universal REDOR curve (as shown in Fig. 2b). It could be due to that ^{1}H–^{13}C dipolar interaction is reintroduced by the soft and hard π pulses during ^{13}C spin selection periods. The strong one-bond ^{1}H–^{13}C dipolar coupling of 13.222 kHz cannot be completely removed by the magic angle spinning of 5 kHz, while for the two-bond ^{1}H–^{13}C of 1.900 kHz (2.1 Å), the residual dipolar interaction during ^{13}C-spin selection periods could be negligible under 5 kHz MAS.

In order to remove the heteronuclear ^{1}H–^{13}C dipolar interaction during the ^{13}C soft pulse periods, we used WIM-24 instead of FSLG to simultaneously remove the homonuclear ^{1}H–^{1}H and heteronuclear ^{1}H–^{13}C dipolar interaction. A soft π pulse of 320 μs put in the middle of REDOR recoupling periods was simulated to investigate the practical experimental situation. As shown in Fig. 2, the REDOR dephasing points in blue are also consistent with the universal dephasing curve. The simulations show that WIM-24 is particularly necessary for measuring strong ^{1}H–^{13}C dipolar couplings, since the suspension of the ^{1}H–^{13}C dipolar interaction during the ^{13}C long π pulse period is crucial. For long-range ^{1}H–^{13}C distances, both FSLG and WIM-24 may work during the ^{13}C selective pulse period.

3.4.2. Effect of homonuclear ^{1}H–^{1}H decoupling

Fig. 3 shows the ^{1}H–^{13}C FS-REDOR dephasing curves in $^{1}\mathbf{H_1}$,$^{1}\mathbf{H_2}$ (CH_2)–$^{13}C_3$ spin system as a function of FSLG decoupling strength. In order to assess the effect of ^{1}H–^{1}H homonuclear decoupling on the ^{1}H–^{13}C FS-REDOR experiment, the universal ^{1}H–^{13}C REDOR dephasing curve for isolated ^{1}H–^{13}C spin pair with distances fixed

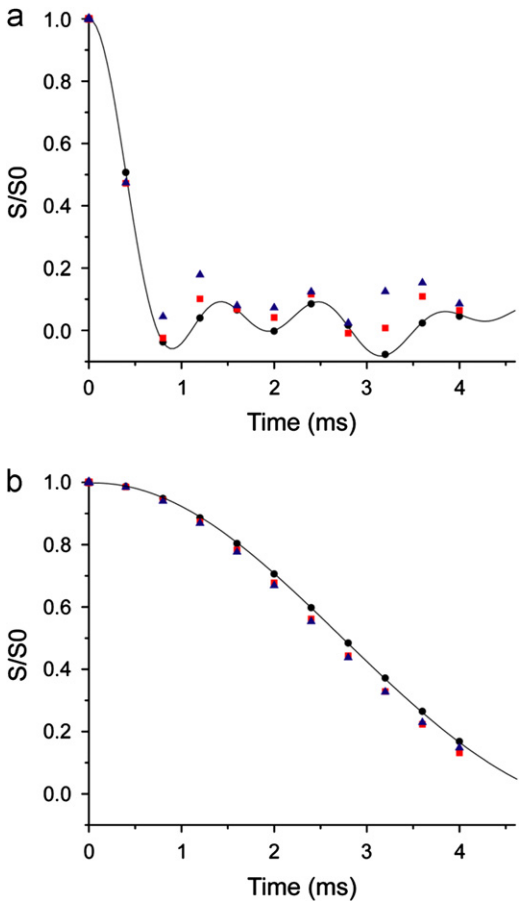

Fig. 3. REDOR simulations on ^{1}H–^{1}H homonuclear decoupling in ^{1}H–^{13}C FS-REDOR experiments. In the simulation program, three-spins system containing $^{1}H_1$, $^{1}H_2$, $^{13}C_3$ with $^{1}H_1$–$^{1}H_2$ distance of 1.45 Å and $^{1}H_{1,2}$–^{13}C distances of 2.1 Å (a) and 4.0 Å (b) were chosen to represent the $^{13}C^{1}H_2$–^{13}C real system. The corresponding control universal REDOR dephasing curves were depicted in black line. The dotted dephasing points (S/S0) in black (circle), red (square) and blue (triangle) denote FSLG decoupling strength setting with 100%, 90%, and 80% accuracy respectively. (For interpretation of the references to color in this figure legend, the reader is referred to the web version of this article.)

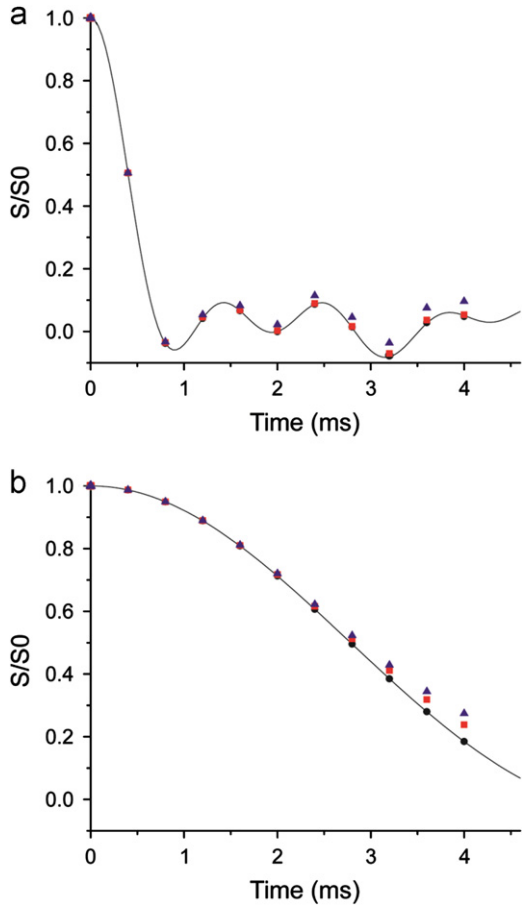

Fig. 4. REDOR simulations on homonuclear ^{13}C–^{13}C J coupling interactions in the ^{1}H–^{13}C FS-REDOR experiment. In the simulation program, four spin system containing $^{1}H_1$, $^{13}C_2$, $^{13}C_3$ and $^{13}C_4$ was selected. $^{1}H_1$–$^{13}C_2$ distances was set to 2.1 Å (a) and 4.0 Å (b). $^{13}C_2$–$^{13}C_3$ J coupling of 35 Hz and $^{13}C_2$–$^{13}C_4$ J coupling of 55 Hz were input in the simulation program. The control universal REDOR dephasing curves were depicted in black line. The dotted dephasing points in black (circle), red (square) and blue (triangle) denote one-bond J-coupling is removed during both the dipolar recoupling and ^{13}C-spin selection periods, only ^{13}C-spin selection periods, and neither dipolar recoupling nor ^{13}C-spin selection period in ^{1}H–^{13}C REDOR experiment. (For interpretation of the references to color in this figure legend, the reader is referred to the web version of this article.)

to 2.1 Å and 4.0 Å after considering the scaling factor of FSLG (theoretical value: 0.577) were also simulated for comparison. The scaling factor of FSLG significantly depends on many experimental variables as reported [44]. According to our previous study [52], the scaling factor of the FSLG was determined to be 0.54 under the similar condition. The universal simulation curves are shown in Fig. 3 in black dotted line. As shown in Fig. 3a, for $^{1}H_1$,$^{1}H_2$–$^{13}C_3$ spin system, the homonuclear ^{1}H–^{1}H dipolar coupling of 22.6 kHz (CH_2 group) and heteronuclear dipolar coupling of 1.900 kHz corresponding to the ^{1}H–^{13}C distances of 2.1 Å were added into the simulation program. As the FSLG decoupling strength meet the LG condition ($\omega_1 = \sqrt{2/3}/P_{\pi,eff}$, $\omega_{off} = \sqrt{1/3}/P_{\pi,eff}$), the simulation dephasing points in blue were exactly consistent with the corresponding isolated spin pair simulation curve. While the FSLG decoupling power is intentionally set slightly off the real FSLG condition with 90% or 80% accuracy, most simulated dephasing points are deviated from the universal dephasing curve, suggesting that the efficient homonuclear ^{1}H–^{1}H decoupling is crucial in the ^{1}H–^{13}C FS-REDOR experiment. The inaccurate set-up of the FSLG would result in not only the incomplete removal of the ^{1}H–^{1}H dipole coupling, but also change the FSLG scaling factor[44] in the ^{1}H–^{13}C FS-REDOR experiment.

The fact is similarly observed for the $^{1}H_1$, $^{1}H_2$–$^{13}C_3$ spin system with a ^{1}H–^{13}C distance of 4.0 Å in Fig. 3b. Generally, to measure the ^{1}H–^{13}C distance between protons from CH_2 group and the neighboring ^{13}C spins, the accurate setting of homonuclear decoupling can remove the homonuclear ^{1}H–^{1}H dipolar interaction as well as eliminate spin diffusion among protons during the ^{1}H–^{13}C REDOR recoupling periods. To improve the homonuclear decoupling in ^{1}H–^{13}C FS-REDOR experiment, one needs to set up the FSLG decoupling condition very carefully or to utilize more advanced homonuclear decoupling schemes [53,54,55] such as DUMBO [56], eDUMBO [57] to effectively remove the homonuclear ^{1}H–^{1}H dipolar interactions.

According to theoretical simulations (data not shown), the heteronuclear ^{1}H–^{15}N, ^{13}C–^{15}N and homonuclear ^{13}C–^{13}C dipolar interactions could also be ignored, such that the heteronuclear dipolar decoupling in ^{15}N channel is not necessary in the ^{1}H–^{13}C FS-REDOR experiment.

3.4.3. *Interference of ^{13}C–^{13}C J coupling*

In order to assess the effect of one-bond ^{13}C–^{13}C *J* interaction in the ^{1}H–^{13}C FS-REDOR experiment, four-spin system including $^{1}H_1$, $^{13}C_2$, $^{13}C_3$ and $^{13}C_4$ was chosen represent ^{1}H–$^{13}C_\alpha$ real system. $^{13}C_2$–$^{13}C_3$ and $^{13}C_2$–$^{13}C_4$ *J* couplings were set to 55 Hz and 35 Hz, respectively. We assume that both the hard and soft ^{13}C π pulse can select $^{13}C_2$ out of $^{13}C_3$ and $^{13}C_4$, it was found that the simulated points are consistent with the universal REDOR dephasing curves (see Fig. 4). While in the practical situation, as

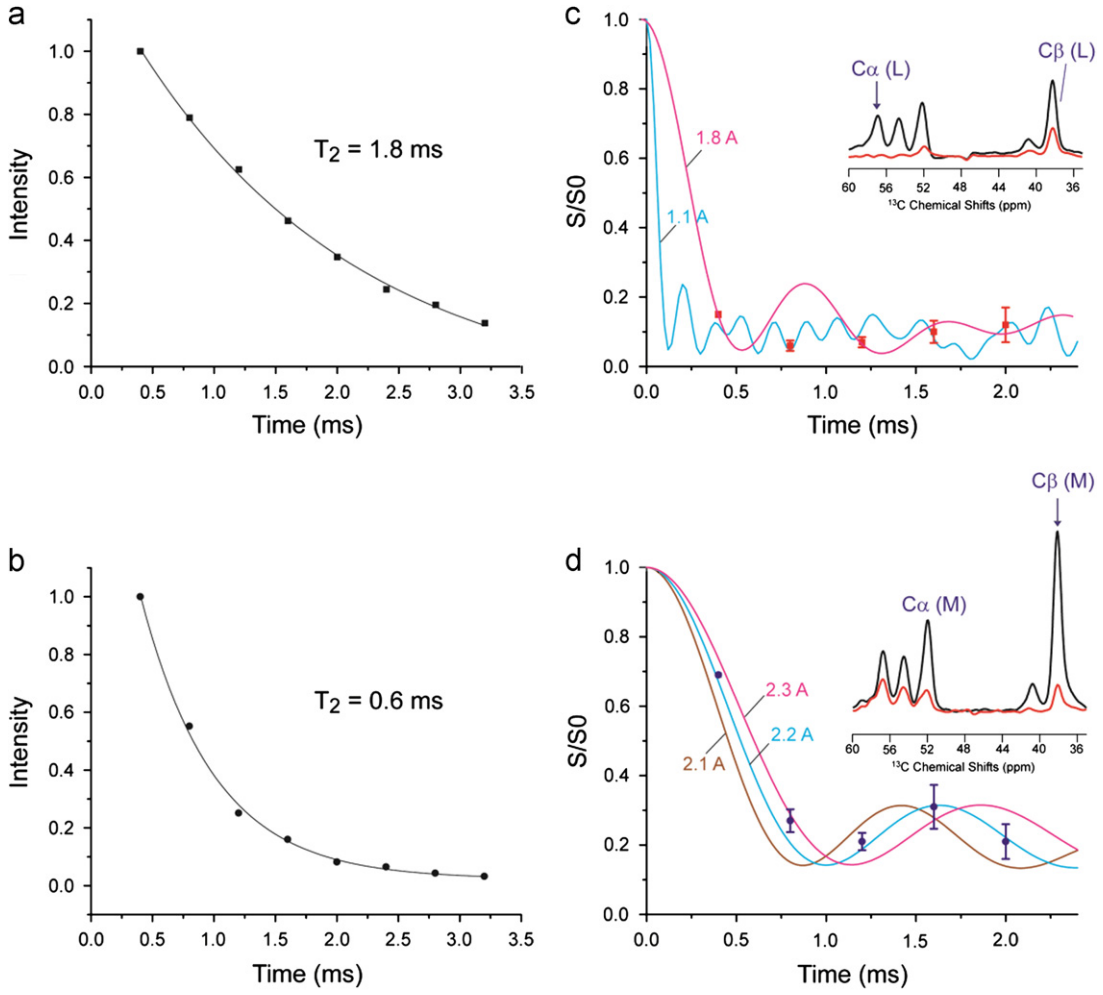

Fig. 5. T_2 values of ^{1}Hα in histidine sample determined from the ^{1}H–^{13}C FS-REDOR experiment as ^{13}C hard π pulses train turned off (a) and turned on (b). Short range intra-residue ^{1}H–^{13}C distances determined from the ^{1}H–^{13}C FS-REDOR experiment. (c) ^{1}Hα–^{13}Cα (Leu) and (d) ^{1}Hα–^{13}Cβ (Met) REDOR dephasing curve in uniformly ^{13}C, ^{15}N labeled MLF sample. The best-fit distances for ^{1}Hα–^{13}Cα (Leu) and ^{1}Hα–^{13}Cβ (Met) is less than 1.8 and ca. 2.2 Å respectively. Calculated REDOR curves are scaled by a factor of 0.92 (c) and 0.83 (d) due to pulse imperfection.

the soft π pulse instead of hard pulse can distinguish $^{13}C_2$ from $^{13}C_3$ and $^{13}C_4$, it was found the simulated points are slightly deviated from the ideal universal REDOR simulation curves at a longer mixing time. Finally, as both the soft π pulse and hard pulse cannot select $^{13}C_2$ from $^{13}C_3$ and $^{13}C_4$, we found that simulated points are deviated off the ideal universal REDOR simulation curves. It reveals that the carbon selective π pulse not only can select the ^{13}C spin of interest but also can partly remove the one bond ^{13}C–^{13}C J coupling interactions. To simultaneously remove ^{13}C–^{13}C J coupling and dipolar interactions and conserve ^{1}H–^{13}C dipolar interaction, C-type symmetry scheme [47,58–60], such as POST-CN_n^{ν} in C-REDOR experiment can be incorporated into the pulse sequence, which is normally used at a faster spinning speed than 20 kHz.

3.5. Experimental demonstration on uniformly ^{13}C, ^{15}N labeled f-MLF and histidine

In the pulse sequence of ^{1}H–^{13}C FS-REDOR experiment as shown in Fig. 1, FSLG, WIM-24 and LG-CP were employed to suppress homonuclear ^{1}H–^{1}H dipolar coupling and avoid spin diffusion during REDOR recoupling and CP polarization transfer periods. In addition, a train of composite π pulses (90°–180°–90°) [61] was used to recouple the heteronuclear ^{1}H–^{13}C dipolar interactions. Moreover, a soft ^{13}C π pulse with pulse length of 320 μs was used to select the ^{13}C spins of interest, which can selectively excite $\pm$6 ppm region around the central selection peak.

In order to evaluate the proton homonuclear dipolar decoupling and ^{1}H–^{13}C heteronuclear recoupling in the ^{1}H–^{13}C FS-REDOR experiment, the intrinsic and apparent T_2 values of $^{1}H\alpha$ were measured. As the hard and soft ^{13}C π pulses were turned off, the instinct T_2 value of $^{1}H\alpha$ of histidine in the ^{1}H–^{13}C FS-REDOR experiment was determined to be around 1.8 ms as shown in Fig. 5a. While as the ^{13}C hard pulses are turned on, the apparent T_2 value in the ^{1}H–^{13}C FS-REDOR experiments were reduced to be around 0.6 ms (see Fig. 5b). The shortened T_2 value could be attributed to imperfect homonuclear decoupling and heteronuclear recoupling or certain systematic error in the ^{1}H–^{13}C FS-REDOR experiment.

For the ^{1}H–^{13}C distance measurements in the uniformly ^{13}C, ^{15}N labeled system, the intermolecular dipolar interruption to short range ^{1}H–^{13}C distances, (e.g. 1.0–2.5 Å), could be ignored compared to intramolecular dipolar interaction. While long range intermolecular distances (3–6 Å) interruption must be avoided. In this work, uniformly ^{13}C, ^{15}N labeled f-MLF and 20% diluted histidine prepared at pH 8.0 were chosen as model compounds to demonstrate the reliability of ^{1}H–^{13}C intramolecular short range and long range distances determination, respectively.

Fig. 5c, d shows the REDOR dephasing curves of short-range intramolecular ^{1}H–^{13}C distances measurements using uniformly ^{13}C, ^{15}N labeled MLF sample. As shown in Fig. 5c, even though the exact $^{1}H\alpha$–$^{13}C\alpha$ distances cannot be deduced from the ^{1}H–^{13}C FS-REDOR experiment due to the lack of initial dephasing points, the one-bond $^{1}H\alpha$–$^{13}C\alpha$ distances can be estimated to be less than 1.8 Å. This distance is consistent with the PDB data (1Q7O) [40]. According to topology structure of MLF, the one-bond ^{1}H–^{13}C distances such as $^{1}H\alpha$–$^{13}C\alpha$ are around 1.07–1.09 Å, while the two-bond ^{1}H–^{13}C distances such as $^{1}H\alpha$–$^{13}C\beta$ are around 2.14–2.16 Å.

Fig. 5d also shows the two-bond $^{1}H\alpha$–$^{13}C\beta$ (Leu) distances simulation curves of MLF. $^{1}H\alpha$–$^{13}C\beta$ distances are determined to be around 2.20 Å, which is in good agreement with the corresponding distances from the PDB file, indicating our method is reliable for the short ^{1}H–^{13}C distance measurements.

In addition to the ^{1}H–^{13}C measurement of distances within two bonds, the long range distances determined using ^{1}H–^{13}C FS-REDOR experiment was investigated as well. Fig. 6b shows the REDOR simulation curves between histidine backbone $^{13}C\alpha$ and sidechain $^{1}H\delta1$ and $^{1}H\varepsilon2$. As shown in Fig. 6b, the distances

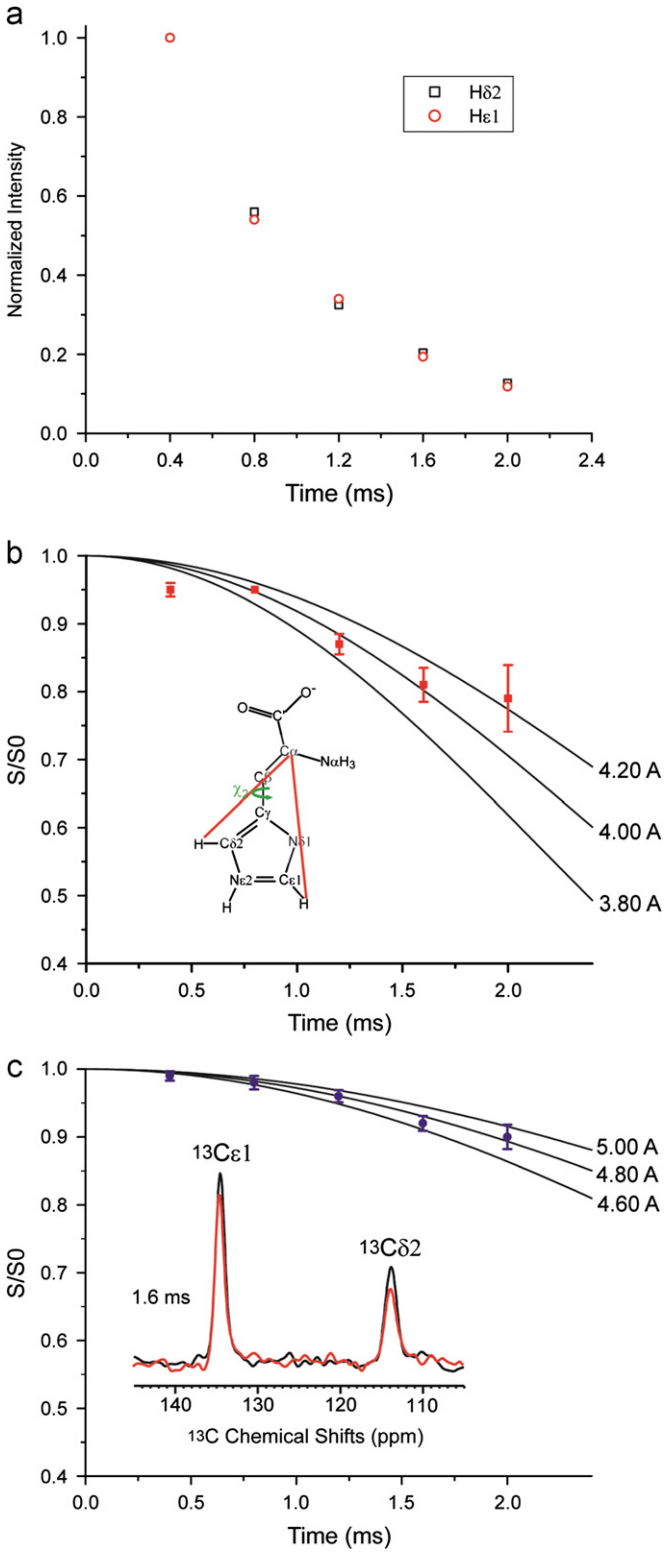

Fig. 6. Long range intra-residue ^{1}H–^{13}C distances determined from the ^{1}H–^{13}C FS-REDOR experiments. (a) The signals decay of $^{13}C\delta2$ and $^{13}C\varepsilon1$ in ^{1}H–^{13}C FS-REDOR experiment. $^{1}H\delta2$–$^{13}C\alpha$ (b) and $^{1}H\varepsilon1$–$^{13}C\alpha$ (c) REDOR dephasing curves in uniformly ^{13}C, ^{15}N labeled histidine sample prepared at pH 8.0 after 20% dilution treatment. According to X-ray data, the $^{1}H\delta2$–$^{13}C\alpha$ and $^{1}H\varepsilon1$–$^{13}C\alpha$ pair distances are estimated to be around 4.15 Å and 4.97 Å respectively.

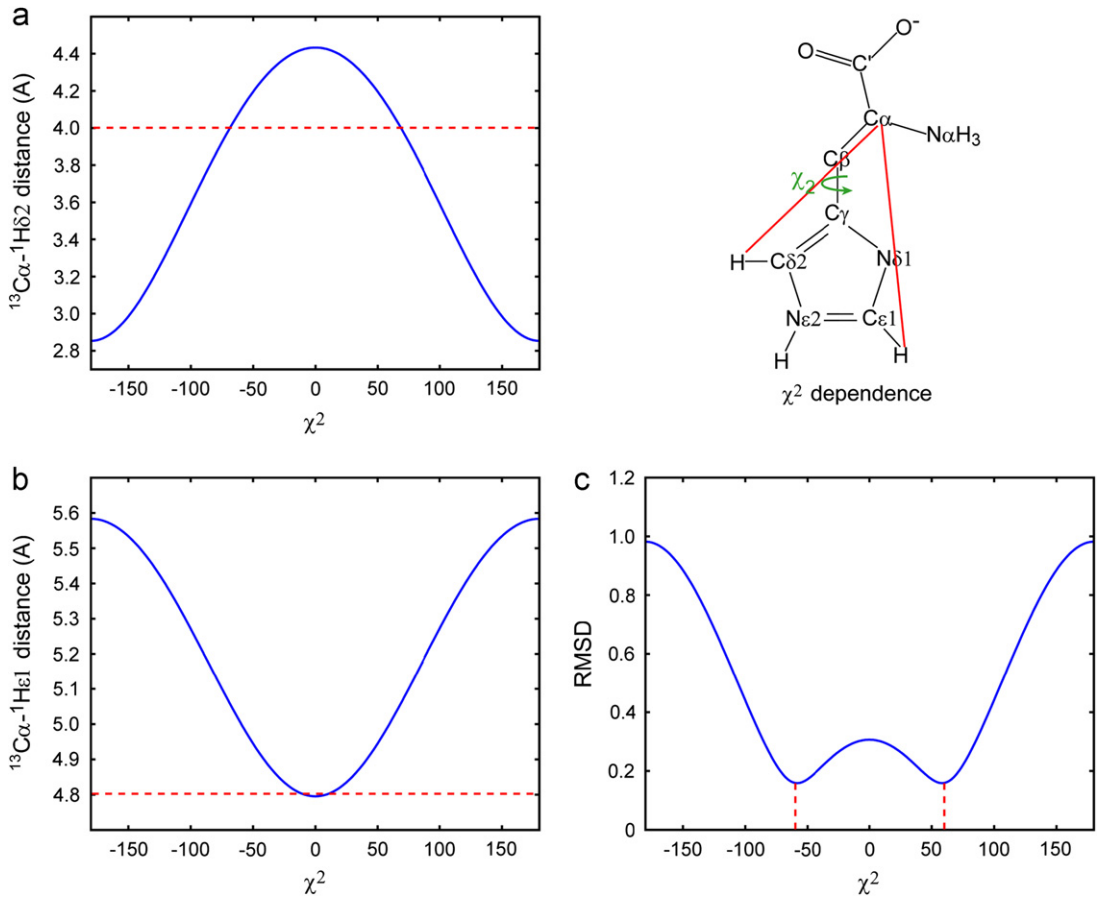

Fig. 7. The simulated distances of ^{1}Hδ2-^{13}Cα and ^{1}Hε1–^{13}Cα and calculated RMSD as a function of the χ2 angle in histidine. The best-fit angles are around -60° and 60°, which is in good agreement with the X-ray data (56.1◦) (CSD code: LHISTD02).

between ^{1}Hδ1 and ^{13}Cα is measured to be 4.0 Å, which agrees well with the X-ray data (4.15 Å) (CSD code: LHISTD02). In addition, the long-range ^{1}Hε1–^{13}Cα distance was measured to be 4.8 Å, which is slightly shorter than the X-ray data of 4.97 Å. Overall, our data shows that the ^{1}H–^{13}C FS-REDOR experiment can successfully measure long range ^{1}H–^{13}C distances up to 5 Å.

Moreover, the intramolecular ^{1}H–^{13}C distances extracted from the ^{1}H–^{13}C FS-REODR experiment could be employed to constrain the sidechain dihedral angle. Fig. 7 plots histidine Hδ2–Cα and Hε1–Cα distances as a function of χ_2 angle according to the crystal structure of histidine [39]. Using the lowest RMSD calculation, we found the best-fit χ2 angle to be about 60° and -60°, in good agreement with the X-ray value of 56.1°. These results imply that the measured intramolecular ^{1}H–^{13}C distances can be used to indirectly give sidechain torsion angles of proteins.

To investigate the 3D structure of proteins, the current ^{1}H–^{13}C FS-REDOR experiment can be served as a supplementary method to obtain the distance and angular constraints for protein structure determinations. In combination with the 2D ^{13}C–^{13}C and ^{13}C–^{15}N correlation methods [62,63], the ^{1}H–^{13}C FS-REDOR can be extended to a 3D mode to yield the distance constraints with high resolution for uniformly labeled proteins.

Since the method can be used to measure the intramolecular ^{1}H–^{13}C and ^{1}H–^{15}N distances for uniformly ^{13}C, ^{15}N labeled proteins, it can also be employed to detect the hydrogen bond in biological proteins. The existence of the hydrogen bonds can be exploited from the long range ^{1}H–^{13}C distance for ^{13}C=O…^{1}H–^{15}N systems in uniformly ^{13}C, ^{15}N labeled proteins. Generally, the hydrogen bond strength can be reflected from the intramolecular ^{1}H–^{13}C distances.

In comparison with ^{13}C–^{15}N FS-REDOR [30] experiment, only one rather than two selective π pulses was present in the ^{1}H–^{13}C FS-REDOR experiment, which allows to obtain lots of sidechain to backbone distances constraints simultaneously. In addition, intramolecular ^{1}H–^{13}C distance in uniformly ^{13}C labeled samples without ^{15}N labeling can also be measured through ^{1}H–^{13}C FS-REDOR experiment.

However, the set-up of ^{1}H–^{13}C FS-REDOR experiment is not as robust as the ^{13}C–^{15}N FS-REDOR [30]. The most possible reason lies in the related short T_2 (0.6 ms) which is strongly subject to the large one-bond ^{1}H–^{13}C dipole interaction in the current ^{1}H–^{13}C FS-REDOR experiment. As is well known, one-bond ^{1}H–^{13}C dipole coupling (22.6 kHz) is more than 20 times that of the ^{13}C–^{15}N dipole coupling (950 Hz). Even though one-bond ^{1}H–^{13}C dipole interaction has negligible influence on the long range ^{1}H–^{13}C distance measurements, it results in the relatively low sensitivity of the ^{1}H–^{13}C FS-REDOR experiment. In addition, to remove the ^{1}H–^{1}H homo-nuclear dipole coupling especially for CH_2 group in ^{1}H–^{13}C FS-REDOR experiment is more difficult than that of strong hetero-nuclear decoupling in ^{13}C–^{15}N FS-REDOR experiment.

4. Conclusion

Intramolecular ^{1}H–^{13}C distance measurements in uniformly ^{13}C, ^{15}N labeled samples were demonstrated in ^{1}H–^{13}C FS-REDOR

experiment. Based on theoretical and simulation analysis, the homonuclear ^{1}H–^{1}H, ^{13}C–^{13}C and heteronuclear ^{1}H–^{15}N, ^{13}C–^{15}N dipolar interactions could be removed, whereas only selected heteronuclear ^{1}H–^{13}C dipolar interactions and one-bond J coupling modulations during the REDOR recoupling periods need to be considered in the ^{1}H–^{13}C FS-REDOR experiment. The intramolecular ^{1}H–^{13}C distance within 5 Å can be quantitatively determined by this technique.

Acknowledgments

This work is supported by an NIH grant, GM066976, to M.H. S.L. is grateful for financial support from the National Basic Research Program of China (2009CB918600) and the National Natural Science Foundation of China (21003154).

References

[1] F. Castellani, B. van Rossum, A. Diehl, M. Schubert, K. Rehbein, H. Oschkinat, Nature 420 (2002) 98–102.
[2] U.H.N. Durr, L. Waskell, A. Ramamoorthy, Biochim. Biophys. Acta 2007 (1768) 3235–3259.
[3] A. Ramamoorthy, Solid State Nucl. Magn. Reson. 35 (2009) 201–207.
[4] A.C. Dedios, J.G. Pearson, E. Oldfield, Science 260 (1993) 1491–1496.
[5] S. Spera, A. Bax, J. Am. Chem. Soc. 113 (1991) 5490–5492.
[6] S.P. Mielke, V.V. Krishnan, Prog. Nucl., Magn. Reson. Spectrosc. 54 (2009) 141–165.
[7] M. Hong, J.D. Gross, R.G. Griffin, J. Phys. Chem. B 101 (1997) 5869–5874.
[8] P.R. Costa, J.D. Gross, M. Hong, R.G. Griffin, Chem. Phys. Lett. 280 (1997) 95–103.
[9] X. Feng, M. Eden, A. Brinkmann, H. Luthman, L. Eriksson, A. Graslund, O.N. Antzutkin, M.H. Levitt, J. Am. Chem. Soc. 119 (1997) 12006–12007.
[10] M. Hong, T.V. Mishanina, S.D. Cady, J. Am. Chem. Soc. 131 (2009) 7806–7816.
[11] T. Gullion, J. Schaefer, J. Magn. Reson. 81 (1989) 196–200.
[12] R.Q. Fu, Chem. Phys. Lett. 376 (2003) 62–67.
[13] L. Chen, X. Lu, Q. Wang, O. Lafon, J. Trebosc, F. Deng, J.-P. Amoureux, J. Magn. Reson. 206 (2010) 269–273.
[14] L. Chen, Q. Wang, B. Hu, O. Lafon, J. Trebosc, F. Deng, J.-P. Amoureux, Phys. Chem. Chem. Phys. 12 (2010) 9395–9405.
[15] Q. Wang, X. Lu, O. Lafon, J. Trebosc, F. Deng, B. Hu, Q. Chen, J.-P. Amoureux, Phys. Chem. Chem. Phys. 13 (2011) 5967–5973.
[16] J.C.C. Chan, H. Eckert, J. Magn. Reson. 147 (2000) 170–178.
[17] D. Huster, X.L. Yao, M. Hong, J. Am. Chem. Soc. 124 (2002) 874–883.
[18] W. Luo, M. Hong, J. Am. Chem. Soc. 128 (2006) 7242–7251.
[19] B.J. van Rossum, C.P. de Groot, V. Ladizhansky, S. Vega, H.J.M. de Groot, J. Am. Chem. Soc. 122 (2000) 3465–3472.
[20] Y. Ishii, J Chem. Phys. 114 (2001) 8473–8483.
[21] A.T. Petkova, Y. Ishii, J.J. Balbach, O.N. Antzutkin, R.D. Leapman, F. Delaglio, R. Tycko, Proc. Natl., Acad. Sci. USA 99 (2002) 16742–16747.
[22] S. Li, Y. Zhang, M. Hong, J. Magn. Reson. 202 (2010) 203–210.
[23] U.H.N. Durr, K. Yamamoto, S.-C. Im, L. Waskell, A. Ramamoorthy, J. Am. Chem. Soc. 129 (2007) 6670–6671.
[24] J. Xu, U.H.N. Duerr, S.-C. Im, Z. Gan, L. Waskell, A. Ramamoorthy, Angew. Chem. Int. Ed. 47 (2008) 7864–7867.
[25] J. Xu, R. Soong, S.-C. Im, L. Waskell, A. Ramamoorthy, J. Am. Chem. Soc. 132 (2010) 9944–9947.
[26] K. Takegoshi, S. Nakamura, T. Terao, Chem. Phys. Lett. 344 (2001) 631–637.
[27] A. Lange, K. Seidel, L. Verdier, S. Luca, M. Baldus, J. Am. Chem. Soc. 125 (2003) 12640–12648.
[28] G. De Paepe, J.R. Lewandowski, A. Loquet, A. Bockmann, R.G. Griffin, J. Chem. Phys. 129 (2008).
[29] R. Ramachandran, V. Ladizhansky, V.S. Bajaj, R.G. Griffin, J. Am. Chem. Soc. 125 (2003) 15623–15629.
[30] C.P. Jaroniec, B.A. Tounge, J. Herzfeld, R.G. Griffin, J. Am. Chem. Soc. 123 (2001) 3507–3519.
[31] C.P. Jaroniec, C. Filip, R.G. Griffin, J. Am. Chem. Soc. 124 (2002) 10728–10742.
[32] R. Janik, X.H. Peng, V. Ladizhansky, J. Magn. Reson. 188 (2007) 129–140.
[33] V. Ladizhansky, R.G. Griffin, J. Am. Chem. Soc. 126 (2004) 948–958.
[34] S. Jehle, M. Falb, J.P. Kirkpatrick, H. Oschkinat, B.-J.v. Rossum, G. Althoff, T. Carlomagno, J. Am. Chem. Soc. 132 (2010) 3842–3846.
[35] A.J. Nieuwkoop, C.M. Rienstra, J. Am. Chem. Soc. 132 (2010) 7570–7571.
[36] K. Schmidt-Rohr, M. Hong, J. Am. Chem. Soc. 125 (2003) 5648–5649.
[37] N. Sinha, M. Hong, Chem. Phys. Lett. 380 (2003) 742–748.
[38] S. Wi, N. Sinha, M. Hong, J. Am. Chem. Soc. 126 (2004) 12754–12755.
[39] S. Li, M. Hong, J. Am. Chem. Soc. 133 (2011) 1534–1544.
[40] C.M. Rienstra, L. Tucker-Kellogg, C.P. Jaroniec, M. Hohwy, B. Reif, M.T. McMahon, B. Tidor, T. Lozano-Perez, R.G. Griffin, Proc. Natl., Acad. Sci. USA 99 (2002) 10260–10265.
[41] J.S. Waugh, L.M. Huber, U Haeberle., Phys. Rev. Lett. 20 (1968) 180–182.
[42] M. Mehring, J.S. Waugh, Phys. Rev. B 5 (1972) 3459–3471.
[43] B.J. v anRossum, H. Forster, H.J.M. deGroot, J. Magn. Reson. 124 (1997) 516–519.
[44] A. Ramamoorthy, Y.F. Wei, D.K. Lee, Annu. Rep. NMR Spectrosc. 52 (2004) 1–52.
[45] A. Bielecki, A.C. Kolbert, M.H. Levitt, Chem. Phys. Lett. 155 (1989) 341–346.
[46] P. Caravatti, L. Braunschweiler, R.R. Ernst, Chem. Phys. Lett. 100 (1983) 305–310.
[47] J.C.C. Chan, Chem. Phys. Lett. 335 (2001) 289–297.
[48] J.C.C. Chan, H. Eckert, J. Chem. Phys. 115 (2001) 6095–6105.
[49] Y. Tian, L. Chen, D. Niks, J.M. Kaiser, J. Lai, C.M. Rienstra, M.F. Dunn, L.J. Mueller, Phys. Chem. Chem. Phys. 11 (2009) 7078–7086.
[50] C.P. Jaroniec, B.A. Tounge, C.M. Rienstra, J. Herzfeld, R.G. Griffin, J. Am. Chem. Soc. 121 (1999) 10237–10238.
[51] M. Bak, J.T. Rasmussen, N.C. Nielsen, J. Magn. Reson. 147 (2000) 296–330.
[52] S. Li, Y. Su, W. Luo, M. Hong, J. Phys. Chem. B 114 (2010) 4063–4069.
[53] E. Vinogradov, P.K. Madhu, S. Vega, New Tech. Solid-State NMR 246 (2005) 33–90.
[54] S.P. Brown, Solid State Nucl. Magn. Reson. 41 (2012) 1–27.
[55] P.K. Madhu, Solid State Nucl. Magn. Reson. 35 (2009) 2–11.
[56] A. Lesage, D. Sakellariou, S. Hediger, B. Elena, P. Charmont, S. Steuernagel, L. Emsley, J. Magn. Reson. 163 (2003) 105–113.
[57] B. Elena, G. de Paepe, L. Emsley, Chem. Phys. Lett. 398 (2004) 532–538.
[58] M. Carravetta, M. Eden, X. Zhao, A. Brinkmann, M.H. Levitt, Chem. Phys. Lett. 321 (2000) 205–215.
[59] A. Brinkmann, M.H. Levitt, J. Chem. Phys. 115 (2001) 357–384.
[60] M.H. Levitt, J. Chem. Phys. 128 (2008).
[61] N. Sinha, K. Schmidt-Rohr, M. Hong, J. Magn. Reson. 168 (2004) 358–365.
[62] E. Crocker, A.B. Patel, M. Eilers, S. Jayaraman, E. Getmanova, P.J. Reeves, M. Ziliox, H.G. Khorana, M. Sheves, S.O. Smith, J. Biomol. NMR 29 (2004) 11–20.
[63] M. Hong, R.G. Griffin, J. Am. Chem. Soc. 120 (1998) 7113–7114.